Original Article
Catalpol improves axonal outgrowth and reinnervation of injured sciatic nerve by activating Akt/mTOR pathway and regulating BDNF and PTEN expression

Huifeng Zhu[1,2], Yuan Wang[1,2], Xian Yang[3], Guoran Wan[4], Yan Qiu[1,2], Xiyue Ye[1,2], Yuqing Gao[1,2], Dong Wan[5]

[1]College of Pharmaceutical Sciences and Traditional Chinese Medicine, Southwest University, Chongqing 400715, China; [2]Engineering Research Center for Chongqing Pharmaceutical Process and Quality Control, Chongqing 400715, China; [3]Department of Pharmacy, The Seventh People's Hospital of Chengdu, Chengdu 610041, China; [4]Class 7 Grade 1, Chongqing Three Gorges Medical College, Chongqing 400016, China; [5]Department of Emergency and Critical Care Medicine, The First Affiliated Hospital of Chongqing Medical University, Chongqing 400016, China

Abstract: *Aim*: This study aimed to investigate the effects of catalpol on sciatic nerve crush injury (SNCI) and further explore the role of Akt/mTOR pathway in its pharmacological efficacy. *Methods*: Mice with SNCI in the right were treated with catalpol. Rapamycin was used to block mTOR signal activation. After sciatic motor nerve function was observed, the gastrocnemius muscles, injury sciatic nerve and spinal cord L4-L6 were isolated. TUNEL staining was done to assess the neuronal apoptosis; Transmission electron microscopy (TEM) was performed to observe the microstructure of regenerated myelinated nerve fibers. The expression of proteins in Akt/mTOR pathway, those related to axon regeneration and cell apoptosis was detected by Western blotting. Brain derived neurotrophic factor (BDNF), phosphatase and tensin homolog deleted on chromosome ten (PTEN), growth associated protein-43 (GAP-43), pro- and anti-apoptosis protein including Bax and BCL-2. *Results*: Catalpol significantly improved the function of injured sciatic motor nerve and facilitated the sciatic motor and sensory nerve fiber growth and the reinnervation of gastrocnemius muscles. TEM showed catalpol increased the density and thickness of regenerated myelinated nerve fibers, which exhibited a regular arrangement. Catalpol significantly reduced the number of apoptotic cells and increased the Bcl-2/Bax ratio in the L4-L6 spinal cord anterior horn. Importantly, catalpol significantly increased the expression of p-Akt, p-mTOR, p-p70S6K, GAP-43 and BDNF, but decreased PTEN expression. Blockade of mTOR activation was partially abrogated by catalpol. *Conclusion*: Catalpol may improve SCNI by enhancing the axonal growth via activating the Akt/mTOR pathway and modulating BDNF and PTEN expression.

Keywords: Catalpol, sciatic nerve crush injury, Akt/mTOR pathway, axon regeneration

Introduction

Peripheral nerve injury may result in severe disability, causing potentially devastating impact on the patient's quality of life and substantially increasing social and personal costs [1]. Unlike the central nervous system (CNS), the peripheral nervous system (PNS) is able to regenerate spontaneously after injury. Theoretically, after a peripheral nerve injury, functional recovery may be achieved if the injured neurons survive and the interrupted axons regrow along the distal stump and re-establish functional connections with its appropriate targets. However, the functional outcomes are often unsatisfactory after peripheral nerve injury, primarily due to the death of neurons and non-neuronal cells in the spinal cord, insufficient axon regeneration, misdirection of regenerating axons and inaccuracy of muscle reinnervation [2, 3]. Thus, it is imperative to develop strategies that can reduce cell death in the spinal cord, promote axonal outgrowth and enhance reinnervation of the denervated targets after peripheral nerve injury.

Naturally, after peripheral nerve injury, the proximal nerve stump will spontaneously regenerate and reinnervate its targets by activating the intrinsic growth capacity of neurons. However,

the intrinsic growth capacity of mature neurons is usually diminished, resulting in suboptimal axonal regeneration. Therefore, to enhance the intrinsic growth capacity of neurons is important for the optimal axonal regeneration in the PNS. It has been shown that the diminished regenerative ability of peripheral nerves is linked to the down-regulation of Akt/mTOR pathway [4]. Genetic up-regulation of mTOR activity in the PNS dorsal root ganglion (DRGs) neurons or adult CNS retinal ganglion cells (RGCs) is sufficient to enhance axonal growth capacity *in vitro* and *in vivo* [4, 5]. However, genetic activation of mTOR in DRGs facilitates axonal regrowth, leading to target innervation defect [4]. Thus, the manipulation of mTOR activity with non-genetic methods may be considered. Although the drugs currently used for nerve regeneration are not available in clinical practice, several agents have been studied to show considerable promise in inhibiting neuronal death and promoting axonal outgrowth after peripheral nerve injury [6-10]. Of interest, pharmacological restriction of the phosphatase and tensin homolog deleted on chromosome ten (PTEN), a negative regulator of mTOR activation, was found to enhance the intrinsic growth of corticospinal tract axons after spinal cord crush injury in mice, and these axons also generated anatomical synapses with appropriate targets [10]. Thus, pharmacological regulation represents a promising strategy for manipulating mTOR activity to achieve functional axonal regeneration. Catalpol is one of the major active components in *Rehmannia* and serves as a marker substance in the chemical evaluation or standardization of *Rehmannia* and its products [11]. In recent decades, a great number of chemical and pharmacological studies have shown that catalpol a member of iridoid glucosides family and its molecular formula is $C_{15}H_{22}O_{10}$ (IUPAC name: β-D-glucopyranoside, (1aS,1bS,2S,5aR,6S,6aS)-1a,1b,2,5a,6,6a-hexahydro-6-hydroxy-1a-(hydroxymethyl)oxireno[4,5]cyclopenta[1,2-c]pyran-2-yl). Catalpol is prevalent in the roots of *Rehmannia glutinosa* and may exert potential therapeutic effects on many diseases, such as diabetes, stroke, Alzheimer's disease and Parkinson's disease [12-17]. Furthermore, catalpol may also act as a pleiotropic neuroprotectant, exerting protective effects on neurons, astrocytes, vascular cells, and oligodendrocytes *in vitro* and *in vivo* [18-23]. In addition, catalpol can modulate Bcl-2 and Bax expression to inhibit neuronal apopto-

sis in the hippocampus after ischemic injury [19], promote axonal growth from neurons, and increase the number of synapses in the ischemic brain. Moreover, catalpol enhances hippocampal neuroplasticity by up-regulating PKC and BDNF expression in aged rats [11]; it also protects forebrain neurons from neurodegeneration and promotes neurite growth by increasing BDNF expression [21]. As shown in our recent study, 5 and 10 mg/kg catalpol improved neurobehavioral outcome of rats after stroke, which was related to the up-regulated GAP-43 and VEGF expression in the brain [12, 23]. Based on available findings, catalpol may exert neuroprotective effects and promote axonal growth in CNS. However, its effects on the peripheral nerve injury and the potential mechanisms remain unclear. The present study aimed to investigate the neuroprotective effects and axonal growth-promoting effects of catalpol in a sciatic nerve crush injury (SNCI) mouse model and further explore the possible of Akt/mTOR pathway in these effects.

Materials and methods

Animals and surgical procedures

Experiments were performed in accordance with Chinese Guidelines for the Care and Use of Laboratory Animals. All protocols were approved by the Animal Experimental Ethics Committee of Southwest University. Adult male Kunming mice weighing 25-30 g were purchased from the Laboratory Animal Center at Chongqing Medical University. Animals were housed for one week and then subjected to SNCI using a previously described method [24], with minor modifications. Briefly, mice were intraperitoneally anesthetized with 3.5% chloral hydrate, and the right sciatic nerve was exposed and clamped at 5 mm proximal to the trifurcation of the sciatic nerve with a pair of sterile forceps (width 2.0 mm), followed by 90° rotation which was remained for 60 sec. The body temperature was maintained at 37°C with a heating pad. During the peri-operative period, animals were housed in controlled conditions with a 12:12 hour light/dark cycle and give *ad libitum* access to food and water.

Drugs and treatments

Catalpol (molecular formula: $C_{15}H_{22}O_{10}$; molecular weight: 362.33 Da) was purchased from Liubobainiao Biotechnology Co., Ltd. (Shijiazhuang,

China); its purity was 99.36% as determined by high-performance liquid chromatography. Mice were divided into five groups: sham group (sham), SNCI group (SNCI), catalpol group (Cat), rapamycin group (Rapa) and rapamycin plus catalpol group (Rapa + Cat). There were 8-10 mice in each group. Catalpol (Cat) was dissolved in normal saline and intraperitoneally administered at 10 mg/kg body weight. Rapamycin (Rapa) was intraperitoneally injected at 5 mg/kg body weight. Mice in the Rapa + Cat group received an intraperitoneal injection of rapamycin 1 h prior to catalpol administration. In the sham group, the sciatic nerve was exposed, but not subjected to crush injury; in the SNCI group, SNCI was introduced, and mice were intraperitoneally injected with an equivalent volume of normal saline. Intraperitoneal injections were performed 1 h before the sciatic nerve was clamped; catalpol injection was repeated once daily for consecutive 7 days; rapamycin injection was performed once daily for consecutive 2 days after surgery. Drug dosages were selected based on previously reported and preliminary experiments [4, 12, 23, 25].

Reagent

Rapamycin was purchased from Bioduly Biotechnology *Co., Ltd.* (Nanjing, China). Acetylthiocholine iodide was purchased from Sigma-Aldrich (St. Louis, MO, USA). Gold chloride was purchased from Adamas Reagent *Co., Ltd.* The terminal deoxynucleotidyl TUNEL bright red apoptosis detection kit was purchased from Vazyme Biotechnology *Co., Ltd.* (Nanjing, China).

Tissue processing

Animals were euthanatized and perfused with cold saline and then with 4% paraformaldehyde in 0.01 M phosphate-buffered saline (PBS; pH 7.35) via the left ventricle on the 7th day after surgery. The bilateral gastrocnemius muscles were collected for further studies, the injured sciatic nerve was then removed, and the L4-L6 segments of the spinal cord were harvested for histological examinations or stored at -80°C for Western blotting. Muscle, nerve and spinal cord samples were also collected from the corresponding level of animals without crush injury and used as controls.

Nerve function examination

On the 7th day after surgery, walking track examination was performed to assess the sciatic nerve function by calculating the sciatic functional index (SFI) as previously described [2, 26, 27]. Briefly, absorbent paper was placed on the floor of the box, and the animal's paws were dipped in ink before it was allowed to walk on the white paper. The print length (PL) and toe-spread distance between toes 1 and 5 (toe spread, TS) were measured with a precision device on bilateral footprints. For PL and TS, the ratio between the injured and the intact paws was calculated, and SFI was calculated as follow: SFI = (-51.2 × PLF) + (118.9 × TSF) - 7.5. In which, PLF = (EPL - NPL)/NPL, TSF = (ETS - NTS)/NTS; where "E" and "N" indicate the injured and the intact hind foot, respectively.

Gastrocnemius muscle weight

On the 7th day after surgery, animals were sacrificed and bilateral gastrocnemius muscles were collected, removed, dried with absorbent filter paper, and then weighed using an analytical balance. The ratio of gastrocnemius muscle weight (right/left, R/L) was calculated using a previously reported method [2] by comparing the wet weight of the muscles from the injured side with the wet weight of the muscles from the contralateral intact side.

Histological analysis

For histological examination, the muscles were embedded in Tissue-Tek O.C.T. Serial 6-μm sections were obtained with Frozen Slicer (Leica CM1900, Germany) and mounted onto poly-lysine-coated slides. Hematoxylin-Eosin (H&E) staining was performed using standard protocols.

Acetylcholinesterase staining

The MEPs expression was investigated in the right gastrocnemius muscles by acetylcholinesterase (AChE) staining with minor modifications [28, 29]. Briefly, fresh gastrocnemius muscles fixed with 4% paraformaldehyde in PBS overnight at 4°C. Cross-sections were obtained through the middle of the muscle, incubated with stock solution (cupric sulfate: 150 mg, glycerin: 190 mg, magnesium chloride: 500

Table 1. Primary antibodies used in this study

Antibody	Antibody	Company	Dilution
PTEN	Rabbit pAb	Beyotime	1:1000
Phospho-PTEN (Ser380)	Rabbit pAb	SBiogot Biotechnology	1:500
Akt	Rabbit pAb	Dingguo, China	1:1000
Phospho-Akt (Ser473)	Rabbit pAb	Beyotime	1:1000
mTOR	Rabbit pAb	Proteintech	1:500
Phospho-mTOR (ser2448)	Rabbit pAb	Cell Signaling Technology	1:1000
p70s6k	Rabbit pAb	Proteintech	1:1200
Phospho-P70S6K	Rabbit pAb	SBiogot Biotechnology	1:500
GAP-43	Rabbit pAb	Proteintech	1:1200
Bax	Rabbit pAb	Proteintech	1:2000
BCL-2	Rabbit pAb	Bioss	1:300
BDNF	Rabbit pAb	Proteintech	1:300
GAPDH	Rabbit pAb	Proteintech	1:5000
β-Actin	Rabbit pAb	Proteintech	1:1000
β-Tubulin	Rabbit pAb	Proteintech	1:1000

Note: pAb: polyclonal antibody.

with 0.1 M PBS (pH 7.2) thrice (3 min for each), and dehydrated in an ascending series of alcohol solutions: 50% alcohol (10 min), 70% alcohol with saturated uranium acetate (12 h) at 4°C, 90% alcohol (10 min), 90% ethanol-acetone (10 min), 90% acetone (10 min), and anhydrous acetone (10 min × 3). Tissues were then embedded in Epon812 ethoxyline resin, cut into ultrathin (100 nm) sections, and stained with uranyl acetate and lead citrate; nerve regeneration was observed under a JEM-1400 transmission electron microscope.

TUNEL staining

Apoptotic cells were detected by TUNEL staining. Briefly, L4-L6 segments of the spinal cord were cut into 10-μm section with frozen slicer (Leica CM1900, Germany). Tissues were fixed with 4% paraformaldehyde in PBS for 1 h and permeabilized with 0.1% Triton X-100 and 0.1% sodium citrate in PBS for 2 min. TUNEL staining was performed according to the manufacturer's instructions. After TUNEL staining, the nucleus was labeled with DAPI. A negative control was created using labeling solution instead of the TUNEL reaction mixture. TUNEL-positive cells were randomly selected from the spinal anterior horn in each section, and a total of 100 cells were counted by a professional observer who was blind to the grouping. The ratio of TUNEL-positive cells to total cells was calculated.

Western blotting

L4-L6 segments of spinal cord were collected, homogenized and lysed in RIPA buffer containing protease and phosphatase inhibitors (Dingguo, China). The protein concentrations were determined using the BCA method. Thirty micrograms of protein were separated on 8-12% SDS-PAGE gels and then transferred onto PVDF membranes (Millipore, HVPPEAC12). The membranes were incubated with Tris-glycine-methanol buffer for 2 h at 4°C. After blocking with 5% bovine serum albumin (BSA), membranes were incubated with different primary antibodies overnight at 4°C. All antibodies were diluted

mg, maleic acid: 900 mg, 4% sodium hydroxide: 15 ml, 40% anhydrous sodium sulfate: 85 ml, and acetylthiocholine iodide: 100 mg) at pH 6.0 and 37°C for 2 h, rinsed with 40% sodium sulfate for 15 min, washed with distilled water for 15 min treated with 20% potassium ferricyanide for 15 min, washed with distilled water for 1 h, dehydrated, and mounted.

Gold chloride staining

The sciatic sensory nerve endings in the right gastrocnemius muscles were examined using the gold chloride staining [30, 31]. Briefly, the tissue was dehydrated in sucrose, treated with a lemon juice solution and then with gold chloride. Tissue samples were embedded in Tissue Tek and sectioned at 80 and 100 μm; sections were directly transferred onto gelatin-coated slides. Slides were processed and mounted. The procedure was performed at both 20-22°C and 30°C with the exception of sucrose dehydration.

Transmission electron microscopy

Three millimeter nerve segments of the distal part of nerve grafts and parallel segments from the control nerves were prefixed with a 4% glutaraldehyde solution and 1.5% paraformaldehyde solution for 2 days at room temperature, rinsed with 0.1 M PBS (pH 7.2) thrice (3 min for each), postfixed in 1% osmic acid and 1.5% potassium ferrocyanide for 1.5 h at 4°C, rinsed
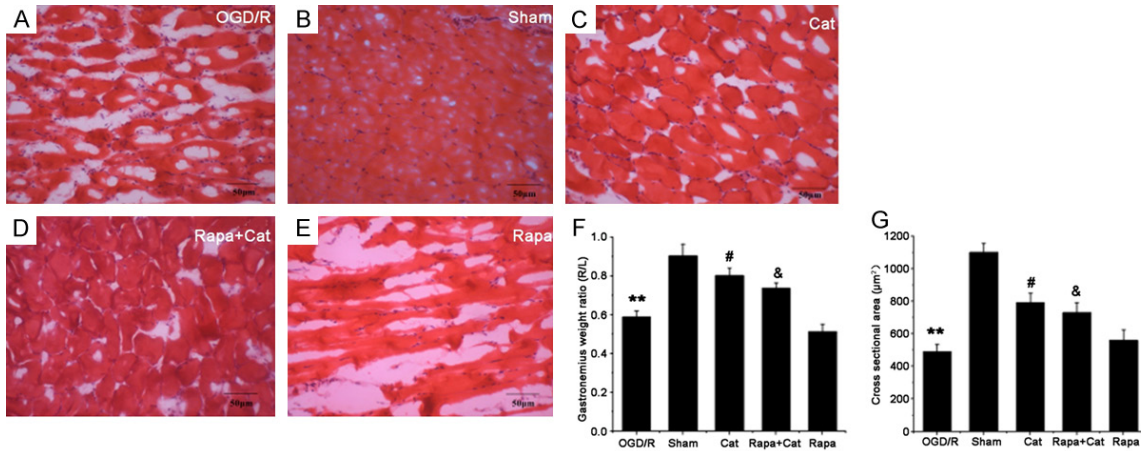
Figure 1. Catalpol protects the gastrocnemius muscle from denervation damage. On the 7th day after SNCI, the pathological changes in the right gastrocnemius muscle were examined by H&E staining (A-E). (F and G) The weight ratio and CSA in the gastrocnemius muscles, respectively. Data are presented as means ± SEM, n=9 mice/group, H&E (200 ×), Scale bar = 50 μm. **$P<0.01$, *$P<0.05$ vs sham group; #$P<0.05$ vs SNCI group; and &$P<0.05$ compared with the Rapa group. Cat = Catalpol, Rapa = rapamycin. #$P<0.05$ vs model group; and &$P<0.05$ vs rapamycin group.

in 5% normal serum in Tris-buffered saline (TBS). The primary antibodies and the dilutions used are listed in **Table 1**. Membranes were rinsed with TBS containing 0.1% Tween 20 (TBST). Proteins were visualized with an enhanced chemiluminescence kit (ECL from GE Healthcare) using peroxidase-conjugated secondary antibodies at 1:5000 (Proteintech). Protein bands were imaged in a Typhoon PhosphorImager (GE Healthcare), and the integrated density of each band was quantified using ImageJ software [32].

Statistical analysis

Data are presented as the means ± standard errors of the means (SEM). Comparisons were done using one-way analysis of variance (ANOVA) followed by post-hoc Tukey test. A value of $P < 0.05$ was considered statistically significant. Statistical analyses were performed using SPSS 17.0 software.

Results

Catalpol promoted motor function recovery of the injured sciatic nerve by activating mTOR

Sciatic nerve injury increased the PL and decreased the TS at the injured side compared with the intact side. The SFI was approximately 0 for non-injured animals and around -100 after the sciatic nerve injury [2]. Based on the SFI, sciatic nerve motor function began to recover 7

days after surgery. The SFI in the sham group (-7.60±2.17) was nearly 0, indicating that nerve function was normal, whereas the SFI in the SNCI group (-88.32±4.19) was only approximately 12% of that in the sham group on day 7 ($P<0.01$). A significantly higher SFI was found in the Cat group (-70.12±1.90) than in the SNCI group ($P<0.05$), suggesting that catalpol mediates a better recovery. However, the catalpol-mediated improvement of functional recovery was remarkably compromised (-77.53±3.38) after mTOR activation was blocked with rapamycin ($P<0.05$), whereas rapamycin alone deteriorated the functional recovery (-90.19±2.80) as compared to the SNCI group ($P<0.05$). Based on these findings, catalpol may promote sciatic nerve motor function recovery after crush injury, which may be related to mTOR activation.

Catalpol prevented denervation of the gastrocnemius muscles by activating mTOR

The weight of muscles distal to an injured and regenerated nerve is proportional to the degree of innervation because the denervated muscles suffer from progressive atrophy, and, this measurement may reflect the functional recovery [2]. In the present study, the reinnervation of the gastrocnemius muscle was examined. The gastrocnemius muscle in the SNCI group displayed serious damage, with cell edema and muscle fiber atrophy, as revealed by the obvious angularity and vacuolization (**Figure 1A**).
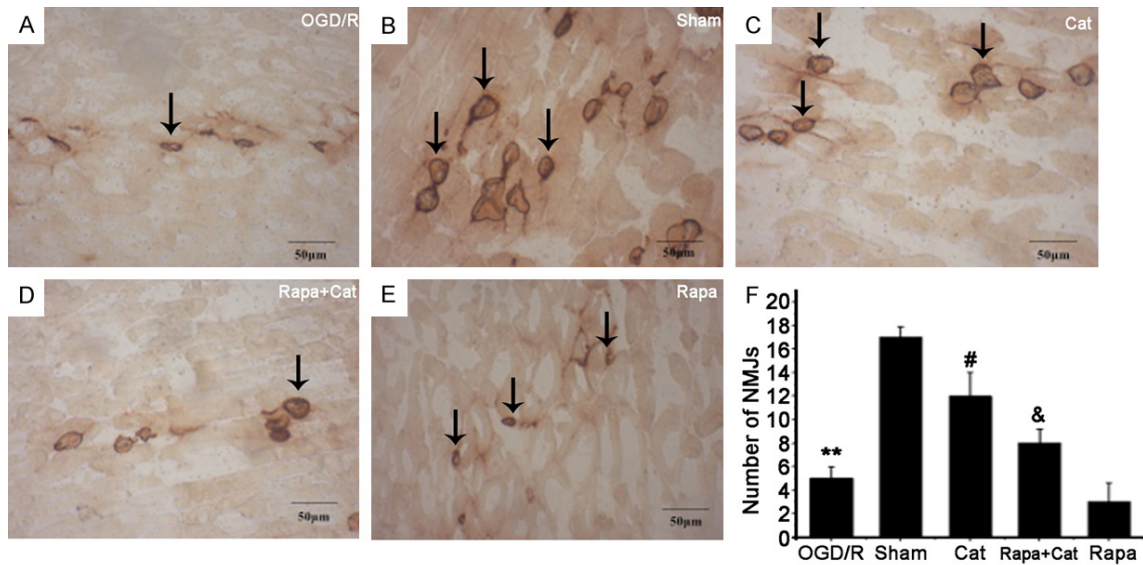
Figure 2. Catalpol increased the number of MEPs in the right gastrocnemius muscles. AChE staining (200 ×). (A) Model, (B) Sham, (C) Catalpol, (D) Rapa + Cat, (E) Rapa. (F) After mTOR blocking with ra-pamycin, the number of MEPs markedly decreased compared with the Rapa + Cat group (P<0.05). Arrows indicate AChE-positive MEPs, Scale bar =50 μm. **P<0.01 compared with the sham group; #P<0.05 compared with the model group; and &P<0.05 compared with the rapamycin group.

However, in the sham group, normal morphological characteristics were observed, and circular and polygonal polynuclei and nuclei located under the surrounding muscle basement membranes (**Figure 1B**). Moreover, catalpol treatment ameliorated the denervation damage to the gastrocnemius muscle; muscle cells were not only closely arranged in neat rows but the number of sarcolemma nuclei within a unit area also increased (**Figure 1C**). However, blockade of mTOR activation by rapamycin partially abrogated the preventive effects of catalpol on the denervation damage to the muscles (**Figure 1D**). Moreover, in the rapamycin group, obvious damage was also observed with muscle cell sarcoplasm dissolution and necrosis as well as interstitial vessel hyperemia (**Figure 1E**). The ratio of gastrocnemius muscle weight confirmed these results (**Figure 1F**). The pathological examination indiates catalpol exerts protective effects on the target muscle reinnervation by the sciatic nerve, which may be related to mTOR activation. We further quantified the cross-sectional area (CSA) of the gastrocnemius muscle fibers in each group (**Figure 1G**) and results showed a significant difference in the CSA between sham group (1102.66±41.46) and model group (498.39±21.46, *P*<0.01). Catalpol significantly increased the CSA (792.19±33.85, *P*<0.05) as compared to the model

group, whereas rapamycin markedly decreased the CSA (587.84±31.64, *P*<0.05). Furthermore, the combination of catalpol and rapamycin yielded a lower CSA (760.77±35.59, *P*<0.05) than catalpol treatment alone. These results confirm the preventive effects of catalpol on the denervation damage and atrophy of the gastrocnemius muscle, which are related to the mTOR activation because rapamycin partially reverses the protective effects of catalpol.

Catalpol increased the reinnervation of target muscles by sciatic motor fibers via activating mTOR

AChE staining is used to examine the morphology of MEPs in the right gastrocnemius muscles, which reflect the nerve terminal endings. The MEPs in the SNCI group showed light blur margin, burr-like morphology, and irregular shapes (**Figure 2A**), which were significantly different from those in the sham group (smooth margin, clear structure and strong staining) (**Figure 2B**). Catalpol increased the number of MEPs with strong AChE staining, and the MEP outline was more complete and nearly resembled MEPs in the sham group (**Figure 2C**). The MEPs in the rapamycin group were sparse and light, and many diffused MEPs (degenerated) were observed (**Figure 2E**). However, the number of stained MEPs in the Rapa + Cat group
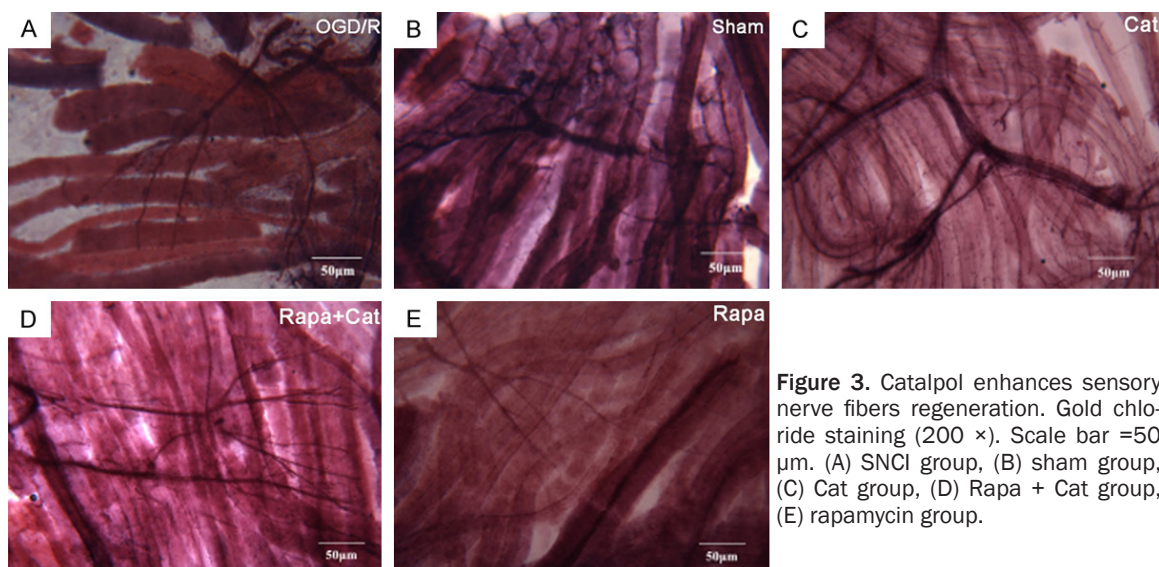
Figure 3. Catalpol enhances sensory nerve fibers regeneration. Gold chloride staining (200 ×). Scale bar =50 µm. (A) SNCI group, (B) sham group, (C) Cat group, (D) Rapa + Cat group, (E) rapamycin group.
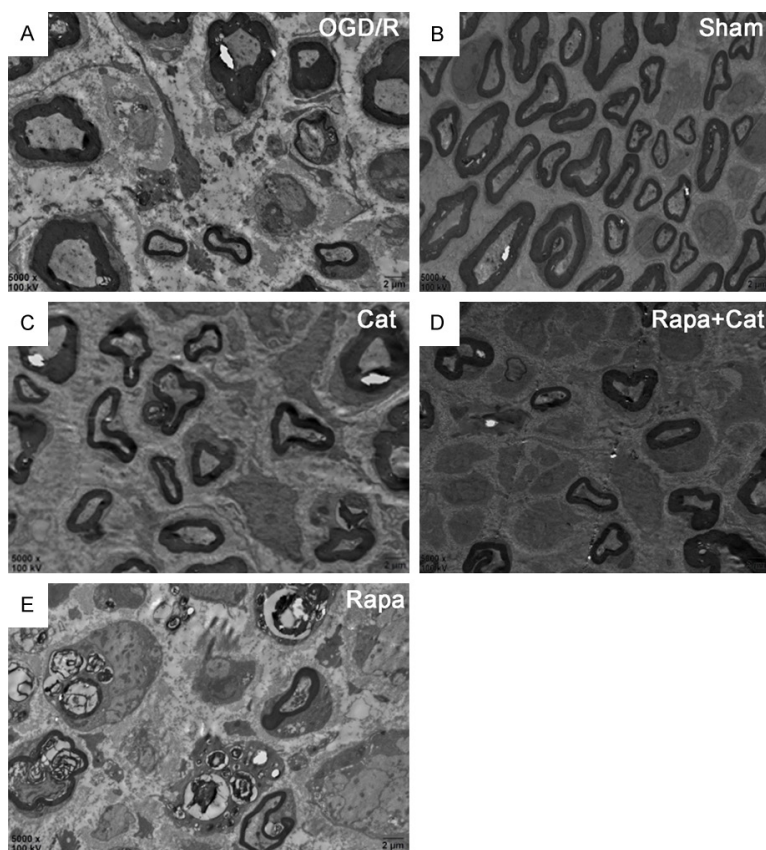

Figure 4. Transmission electron microscopy images of the sciatic nerves in each group (5000 ×), scale bar: 2 µm. (A) SNCI group, (B) sham group, (C) Cat group, (D) Rapa + Cat group, (E) rapamycin group. Sciatic nerve axons were wrapped by thin layers of myelin after crush injury, and catalpol reversed this phenomenon, as thicker layers of myelin were observed. Rapa aggravated myelin injury, and more debris and demyelination were observed. Catalpol reversed the effects of Rapa on the myelination.

slightly increased compared with the SNCI group or the rapamycin group (**Figure 2D**). Moreover, fewer MEPs were observed in the SNCI group than in the sham group (4.73± 0.92 *vs* 17.10±0.87, *P*<0.01). Furthermore, catalpol markedly increased the number of MEPs compared with the SNCI group (11.94±0.74, *P*<0.05). After mTOR blocking with rapamycin, the number of MEPs markedly decreased compared with the Rapa + Cat group (2.88±0.34 *vs* 8.40± 1.78, *P*<0.05) (**Figure 2F**). Based on these findings, catalpol significantly increases the MEPs reinnervation and mTOR activation, leading to the increased sciatic motor axonal growth.

Catalpol enhanced sensory nerve fiber outgrowth and reinnervation by activating mTOR

The gold chloride staining was employed for the examination of myelinated axons and sensory nerve endings in the right
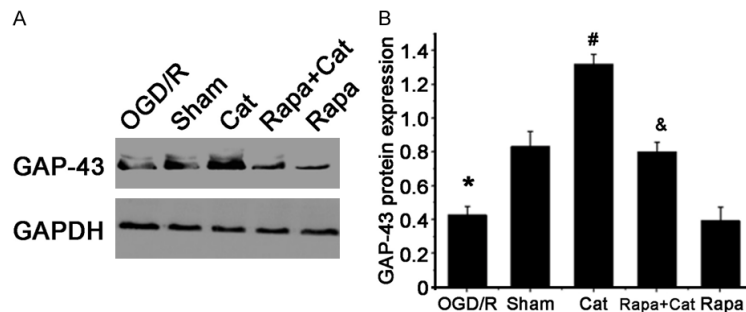
Figure 5. Western blotting shows catalpol-mediated up-regulation of GAP-43 expression in the L4-L6 segments of the spinal cord. A. Western blotting of GAP-43 protein in the L4-L6 segments of the spinal cord; GAPDH served as a loading control. B. Quantitative analysis of the ratio of GAP-43 to GAPDH. Data are presented as means ± SEM. n=9 mice/group. *P<0.05 vs sham group; $^\#$P<0.05 vs SNCI group; and $^\&$P<0.05 vs Rapa group.

number of nerve fibers were observed (**Figure 4B**). In the Cat group, denser and thicker regenerated myelin sheath, increased nerve fibers and irregular arrangement of regenerated myelin sheath were observed compared with the SNCI group (**Figure 4C**). In the rapamycin group, thin, irregular, blurred and broken myelin sheathes were observed (**Figure 4E**), but catalpol also reversed the rapamycin-induced changes in the myelin sheathes (**Figure 4D**).

gastrocnemius muscles, and significant difference was observed in the pattern of sensory innervation among groups. In the sham group, the muscle fibers were light reddish purple and transparent, and showed distinct cross striations; the nerve fibers and their endings were stained deep purple black with no segmentation of the axonal materials (**Figure 3B**). However, in the SNCI group, a light pink background was observed, and the nerve endings had a claw-like appearance (**Figure 3A**). In the Cat group, a clear axonal tree-like structure with more terminal branches were observed, and the intertwined cylindrical sensory nerve endings were stained dark purple. Moreover, the intramuscular nerve branches clearly displayed the typical tube-like appearance (**Figure 3C**). In contrast, in the Rapa + Cat group, a greater number of elongated nerve fibers displayed sparse endings (**Figure 3D**). Similarly, in the rapamycin group, nerve fibers were stained pink with a filamentous-like appearance and rare endings (**Figure 3E**). These findings indicate that catalpol enhances sciatic sensory nerve fiber outgrowth and reinnervation, in which mTOR plays an important role.

Catalpol improved the regeneration of the myelin sheath by transmission electron microscopy

In the SNCI group, blurry myelin sheaths were observed around the medullary nerve fibers and exhibited a lamellar structure, increased spaces and cavities, and sparse alignment (**Figure 4A**). However, in the sham group, the arrangement and thickness of medullary nerve fibers were regular and uniform, and a typical

Catalpol up-regulated GAP-43 expression via mTOR

GAP-43 is a crucial regulator of axonal outgrowth in the developing and regenerating neurons. In the present study, western blotting was performed to detect the GAP-43 expression in L4-L6 segments of the spinal cord. GAP-43 expression was significantly higher in the Cat group (1.31±0.39) than in the SNCI group (0.42±0.11) and sham group (0.85±0.30). Rapamycin significantly decreased the GAP-43 expression (0.40±0.21), and rapamycin suppressed the catalpol-mediated increase in GAP-43 expression (0.81±0.33) (**Figure 5A** and **5B**). Based on these results, we concluded that catalpol up-regulated the GAP-43 expression in the spinal cord connected to the injured sciatic nerve, which is dependent on the mTOR activation.

Catalpol inhibited apoptosis by activating mTOR

The cytoprotective effects of catalpol were investigated by TUNEL staining (**Figure 6A** and **6B**). A remarkable decrease in the number of apoptotic cells (TUNEL-positive cells) was found in the spinal anterior horn of catalpol-treated animals at 1 week post-injury compared to the Rapa + Cat and Rapa groups, indicating that catalpol inhibited apoptosis by activating mTOR. Western blotting was employed to detect the expression of pro-apoptotic Bax and anti-apoptotic BCL-2 in the L4-L6 segments of the spinal cord and results confirmed the inhibitory effects of catalpol on cell apoptosis (**Figure 6C** and **6D**). Catalpol increased the BCL-2/BAX
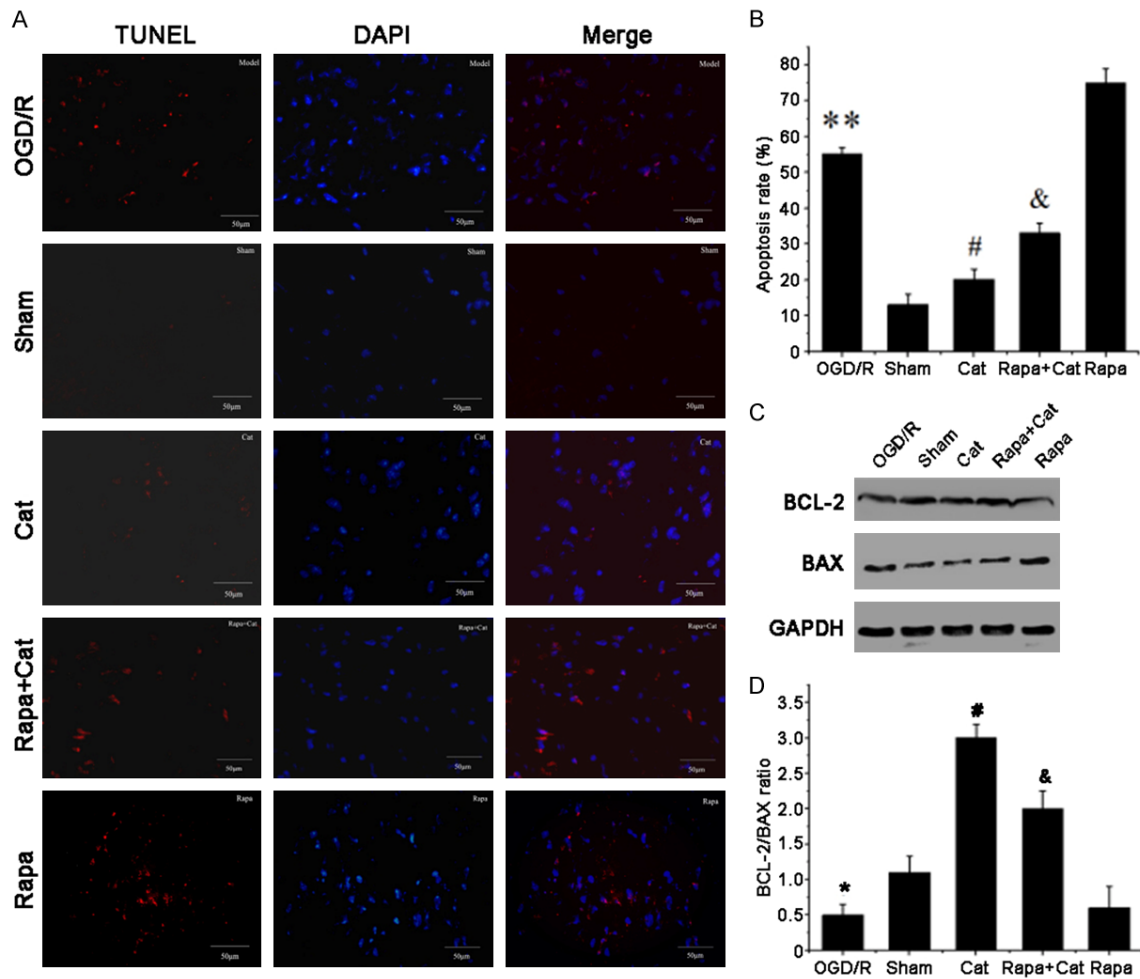
Figure 6. Catalpol inhibits apoptosis and increases BCL-2/BAX ratio by activating mTOR. A. Cell apoptosis was detected in the L4-L6 segments of the spinal anterior horn by DAPI (*blue*) and TUNEL (*red*) double staining. B. Quantitative analysis of TUNEL-positive cells. C. Western blotting for BCL-2 and BAX expression; GAPDH served as a loading control. D. BCL-2 to BAX ratio. Data are presented as means ± SEM, n=9 mice/group, Scale bar =50 μm. $^{**}P<0.01$, $^{*}P<0.05$ vs sham group; $^{#}P<0.05$ vs SNCI group; and $^{&}P<0.05$ vs rapamycin group.

ratio and inhibited cell apoptosis, which was related to the mTOR activation.

Catalpol activated the Akt/mTOR pathway

The effects of catalpol on the Akt/mTOR pathway were further investigated in which the expression of p-Akt/Akt, p-mTOR/mTOR and p-p70S6K/p70S6K was detected. As shown in **Figure 7A** and **7D**, catalpol induced a 117.14% increase in phosphorylated mTOR (p-mTOR) compared to the SNCI group (1.52±0.39 *vs* 0.70±0.24, *P*<0.05). However, the catalpol-induced increase in p-mTOR was partially abrogated by rapamycin, and the rapamycin alone remarkably blocked mTOR phosphorylation, indicating that catalpol activates mTOR. The

p70 ribosomal protein S6 kinase (p70S6K) is a crucial downstream effector of mTOR, and p-p70S6K usually serves as an indicator of mTOR activation. As shown in **Figure 7B** and **7E**, catalpol dramatically increased p-p70S6K expression compared with the SNCI group, whereas blockade of mTOR activation with rapamycin diminished the effects of catalpol, and rapamycin alone significantly reduced the p-p70S6K/ p70S6K ratio. This confirms catalpol induced mTOR activation. Furthermore, the effects of catalpol on the expression of Akt, an important upstream regulator of mTOR, were investigated to determine whether catalpol directly or indirectly modulates mTOR activity. In the SNCI group, the expression of total Akt (t-Akt) and phosphorylated Akt (p-Akt) reduced compared
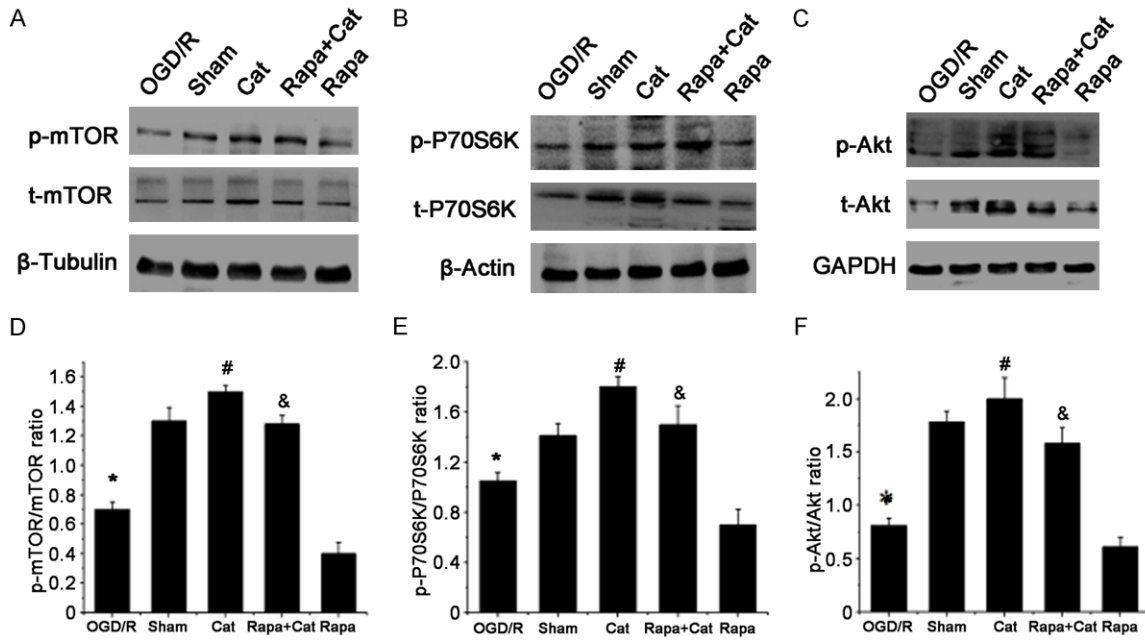
Figure 7. Catalpol activates the Akt/mTOR/p70S6K pathway. Western blotting shows the expression of (A) total mTOR (t-mTOR), phosphorylated mTOR (p-mTOR), (B) P70S6K, phosphorylated P70S6K (p-P70S6K), (C) Akt and phosphorylated Akt (p-Akt) in each group; β-tubulin, β-actin and GAPDH served as loading controls. Quantification of (D) mTOR, (E) P70S6K and (F) Akt activation. Data are presented as means ± SEM. n=9 mice/group. *P<0.05 vs sham group; #P<0.05 vs SNCI group; and &P<0.05 vs Rapa group.
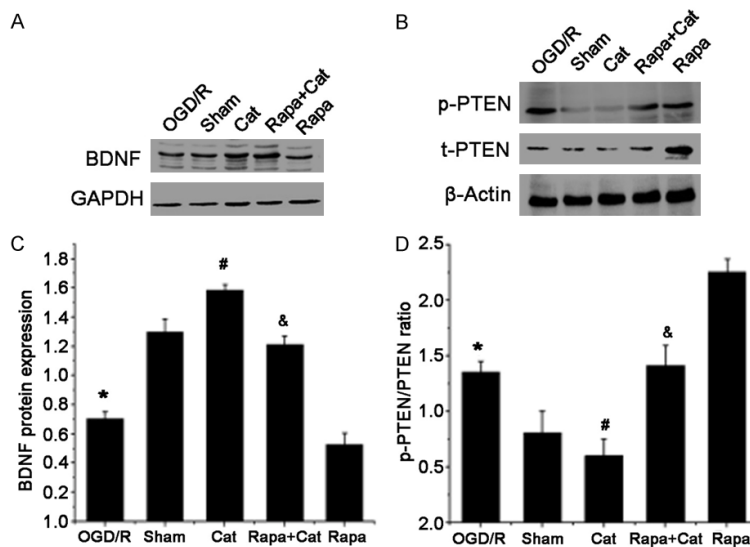

Figure 8. Catalpol modulates BDNF expression and PTEN activation. Western blotting of (A) BDNF, (B) total PTEN (t-PTEN) and phosphorylated PTEN (p-PTEN) expression in the L4-L6 segments of the spinal cord in each group; GAPDH and β-actin served as loading controls. Quantification of (C) BDNF and (D) the p-PTEN to t-PTEN ratio. Data are presented as means ± SEM n=9 mice/group. *P<0.05 vs sham group; #P<0.05 vs SNCI group; &P<0.05 VS Rapa group.

with the sham group, whereas catalpol induced 168.83% increase in p-Akt as compared to the SNCI group. Of interest, catalpol-induced p-Akt

activation was not abrogated by rapamycin-induced mTOR blockade, whereas rapamycin alone significantly reduced the p-Akt expression (**Figure 7C** and **7F**), suggesting the Akt is an important target of catalpol. These findings indicate catalpol activates the Akt/mTOR pathway.

Catalpol modulated BDNF expression and PTEN activation

Akt can be activated by multiple factors (such as BDNF and PTEN) to either inhibit or activate mTOR. PTEN is a negative regulator of Akt/mTOR activity, whereas BDNF is a positive regulator of this pathway. We hypothesized that catalpol could affect Akt/mTOR activity by modulating BDNF and PTEN expression. As expected, catalpol significantly increased BDNF expression in the spinal cord: an approximately 2-fold increase in the BDNF expression after catalpol treatment compared with the

SNCI group and an 0.2-fold increase compared with the sham group. In addition, the catalpol-induced increase in BDNF expression was slightly diminished after the blockade of mTOR activity with rapamycin (**Figure 8A** and **8C**). Moreover, PTEN phosphorylation was substantially inhibited by catalpol, but total PTEN (t-PTEN) and phosphorylated PTEN (p-PTEN) expressions significantly increased after mTOR activation was blocked with rapamycin, which were partially reversed by catalpol (**Figure 8B** and **8D**).

Discussion

Our findings indicate the Akt/mTOR pathway is activated in the L4-L6 spinal cord connected to the injured sciatic nerve, and the blockade of mTOR activation with rapamycin diminishes the growth capacity of sciatic nerve axons and impeds neural functional recovery following SNCI, suggesting that mTOR activation contributes to spontaneous axonal growth. Histological, morphological, and neurological examination reveal that catalpol prevents cell apoptosis in the L4-L6 segments of the spinal anterior horn and promotes sciatic sensory and motor nerve fiber regrowth and functional recovery after crush injury. Furthermore, catalpol activates the Akt/mTOR pathway because blockade of mTOR with rapamycin partially abrogates the pharmacological effects of catalpol. In addition, catalpol regulates BDNF and PTEN expression in the spinal segments connected to the injured sciatic nerve.

Theoretically, functional deficits following peripheral nerve injury are reversed or compensated in a permissive environment, and spontaneous axonal regeneration occurs in the PNS [2]. However, the apoptosis of neuronal and non-neuronal cells and the decreased ability to regenerate axons in adults lead to an insufficient number of axons, and some of the regenerating axons fail to generate connections with appropriate targets [4]. Thus, many patients with peripheral nerve injury exhibit incomplete long-term recovery, often with partial or total loss of motor, sensory, and autonomic function as well as intractable neuropathic pain. Although several pharmacological agents and non-pharmacological methods have been explored and tested in cells and animal models of peripheral nerve injuries [1, 6], the current clinical therapies are largely ineffective in restoring functional recovery. Hence, studies aim to identify new strategies, including drugs that both reduce neuronal death and promote axonal outgrowth, that are essential to reverse the neurological deficit after peripheral nerve injury or a disease.

The sciatic nerve, which comprises a mixed population of motor and sensory axons, is a widely used in peripheral nerve regeneration studies. When a focal injury is superimposed on the nerve, it may exhibit severe regenerative failure with slowing motor and sensory recovery after 1 week. In this study, the mouse model of SNCI was established to observe the effects of catalpol on the axonal regrowth and the functional prognosis of sciatic nerve injury. If the sciatic nerve is injured, its target muscle usually becomes atrophic due to denervation. Conversely, if the muscle is reinnervated, muscle atrophy may be improved with the functional recovery [33]. Our results showed catalpol significantly inhibited the gastrocnemius muscle atrophy; the muscle weight recovered to 61% of that in the sham group and was significantly higher than in the SNCI group ($P<0.05$). Furthermore, the CSA of the gastrocnemius muscle fibers was determined in each group, and results confirmed above findings. This indicates catalpol is able to protect against muscle atrophy and improves muscle function. Above findings indicate catalpol may promote sciatic nerve regrowth and target muscle reinnervation after injury.

In our study, SFI was used to determine whether catalpol affected the regeneration of the sciatic nerve, because it is closely related to the motor function recovery and the morphological and morphometric regeneration of peripheral nerves following injury [34]. Results showed catalpol significantly improved the neuromuscular function which was better than in the SNCI group ($P<0.05$). Moreover, the gastrocnemius muscle weight ratio was highly correlated with the SFI, indicating that the improvement of the gastrocnemius muscle weight was attributed to appropriate reinnervation. Functional recovery is an important outcome of successful peripheral nerve regeneration; thus, based on our results, catalpol exerts beneficial effects on the nerve regeneration.

In addition, AChE staining was used to display MEPs [29], and gold chloride staining was employed to examine the myelinated axons and sensory nerve endings in the targets [30, 31]; thus, the arrival of regenerating axons at the distal target muscles and subsequent reinnervation can be further investigated [2]. Since MEPs are the physiological interface between motor neurons and muscle fibers, MEPs within a muscle indirectly reflect motor nerve fibers and muscle innervation [29]. In the present study, the crushed sciatic nerve exhibited a significantly reduced number of MEPs, and thinner axons and/or fewer nerve endings were also observed after gold chloride staining. However, catalpol reversed these changes induced by crush injury: the number of MEPs and sensory nerve endings increased in the target muscles. The findings also confirmed the change in SFI, suggesting that catalpol contributes to the sciatic nerve axonal regeneration and target muscle reinnervation after injury.

TEM was used to observe the structure of regenerated nerve fibers. 7 days later, serious crush nerve injury was still observed in the SNCI group, as shown by sparse and fewer numbers of regenerated myelinated nerve fibers. However, in the Cat group, dense and regularly arranged fibers were observed, and catalpol reversed the deterimental effects of rapamycin on the repair of nerve crush injury, suggesting that catalpol promotes the regeneration of myelinated nerve fibers after crush injury.

Because successful axon regeneration is achieved only if the injured neurons survive and restore function after injury, we focus on the central surviving cells in the L4-L6 spinal cord connected to the injured sciatic nerve, where a large number of injured motor neurons are undergoing apoptosis [8, 9]. Generally, a large amount of axon growth-associated proteins are produced at the cell body and transported back to the tip of the regrowing axons [35]. Both cell survival and protein synthesis are linked to the prognosis following nerve injury. In the present study, TUNEL staining showed a large number of apoptotic cells in the L4-L6 spinal anterior horn after SNCI, accompanied by down-regulation of anti-apoptotic BCL-2 and up-regulation of pro-apoptotic BAX. These are consistent with previously reported in animal models [8, 9].

However, catalpol significantly reduced apoptosis and concomitantly modulated the BCL-2/BAX ratio to inhibit apoptosis by up-regulating BCL-2 and down-regulating BAX. Meanwhile, mTOR blockade by rapamycin partially diminished the anti-apoptotic effects of catalpol. These findings suggest catalpol inhibit apoptotic cell death in the L4-L6 spinal cord after SNCI, which is closely related to mTOR activation. GAP-43 expression was detected by Western blotting to further examine the ability of surviving cells to synthesize axon growth-associated proteins. GAP-43 is an intrinsic factor required for the axonal regeneration and a sensitive and specific marker of nerve repair that plays an important role in the nerve growth, development and regeneration [36, 37]. GAP-43 expression was down-regulated in the L4-L6 spinal cord after SNCI, which may account for the poor spontaneous axonal growth. However, catalpol strikingly increased the GAP-43 expression and exerted beneficial effects on the motor and sensory nerve regrowth, whereas mTOR blockade with rapamycin partially abrogated the effects of catalpol. Based on these results, catalpol not only reduces cell death but also promotes the synthesis of axon growth-associated proteins through mTOR activation.

The mTOR protein is required for cell proliferation, survival, and axon regrowth [38]. Activation of mTOR leads to the activation of its downstream effector p70 ribosomal protein S6 kinase (p70S6K), further initiating the translation of other proteins, such as GAP-43 [4]. Our study showed a decrease in mTOR activation in the L4-L6 spinal cord on the 7th day after sciatic nerve injury, which might be related to the poor axonal growth. These results were consistent with previous findings that mTOR activation is required for the effective and timely regeneration of peripheral nerves in the PNS [4, 39] or forthe regenerative axonal growth in the CNS [5]. Catalpol significantly enhanced mTOR activation, accelerated axonal regeneration and concomitantly improved target muscle reinnervation, suggesting that mTOR plays a vital role in the catalpol-mediated sciatic nerve regrowth and prevention of muscle atrophy. Rapamycin was used to block mTOR activation in an effort to further determine whether catalpol-induced axonal regrowth depends on mTOR activation. Our results showed rapamycin partially dimin-

ished the catalpol-induced axonal growth, suggesting that mTOR activation contributes to the catalpol-mediated increase in the regenerative potential after sciatic nerve injury.

Although catalpol activates mTOR in the spinal cord after SNCI, the mechanism by which catalpol modulates mTOR activity remains still unclear. Akt is a critical upstream regulator of mTOR, and Akt activation may lead to mTOR activation. Therefore, we hypothesized that catalpol altered Akt phosphorylation, and at least partially modulated mTOR activation by targeting its upstream regulators. Our results showed Akt activation was suppressed in the L4-L6 spinal cord after SNCI, which was consistent with previous findings that Akt activation was altered in the distal segment of nerves and sensory neurons, and a number of Akt targets, including mTOR and S6, are also down-regulated after sciatic nerve injury [38]. However, catalpol markedly activated Akt, which was partially abrogated by rapamycin. Consistent with our results, catalpol was also found to activate the Akt signaling pathway in oligodendrocyte progenitors [40] and human endothelium [41]. Thus, Akt is another target of catalpol.

Akt integrates a plethora of essential signaling pathways in response to diverse stimuli, such as growth factors, nutrients, ATP, and reactive oxygen species, to control mTOR activation [42]. BDNF is required for neuron survival and nerve regeneration [43]. The binding of BDNF to its TrkB receptor positively regulates Akt activity through phosphoinositide 3-kinase (PI3K) and subsequently mTOR. In the present study, the BDNF expression significantly decreased in the L4-L6 spinal cord, whereas catalpol markedly up-regulated BDNF expression. Similar to observations in CNS neurons, catalpol also promotes BDNF expression to increase neurite outgrowth *in vivo* and *in vitro* [21]. Based on these findings, catalpol likely induces mTOR activation via activating PI3K/Akt pathway by increasing BDNF expression.

Although neurotrophic factors are required to activate Akt/mTOR pathway, negative modulatory factors are also required for the fine control of Akt/mTOR activity. PTEN is a negative modulatory factor and upstream target of the Akt/mTOR pathway; PTEN activation leads to a decrease in mTOR activity [44]. Inhibition of PTEN through either pharmacological blockade or local siRNA facilitates the intrinsic regenerative outgrowth of adult peripheral axons [44, 45], and initiates the regrowth of injured CNS axons by activating mTOR [5]; PTEN might act as an intrinsic brake on the regenerative outgrowth [45]. As shown in our study, PTEN was prominently expressed in the L4-L6 spinal cord after sciatic nerve injury, and catalpol significantly down-regulated the PTEN expression and activation, which accounted for the catalpol-mediated activation of Akt/mTOR pathway. To our surprise, PTEN expression significantly increased and p-Akt expression remarkably decreased by rapamycin, which may be explained by the negative feedback loop of mTOR-S6K1 pathway to the upstream PTEN-PI3K/Akt cascade [46, 47], but the exact mechanism remains to be further elucidated.

Based on our results, catalpol ameliorates the denervation and atrophy of the gastrocnemius muscles, enhances sciatic motor and sensory nerve fiber outgrowth and target reinnervation, and subsequently improves sciatic nerve motor function after injury. In addition to promoting axonal growth, catalpol also effectively inhibits apoptosis in the L4-L6 segments of the spinal cord anterior horn. These effects are linked to mTOR activation since blockade of mTOR activation with rapamycin partially abrogates the effects of catalpol. Meanwhile, catalpol activates the Akt/mTOR pathway, up-regulates BDNF expression and down-regulates PTEN expression. Modulation of BDNF and PTEN expression by catalpol may underlie its activation of the Akt/mTOR pathway. These findings suggest catalpol may become a potential drug for the treatment of peripheral nerve injury. However, there were still limitations in the present study. The alterations in the spinal cord and the target muscle of sciatic nerve were observed, but the changes in the proximal and distal nerve stumps were not investigated. Although catalpol effectively promoted axonal outgrowth, we did not distinguish among axonal regeneration, sprouting and remodeling. In addition, the mechanism by which catalpol activates the Akt/mTOR pathway remains still unclear. Furthermore, the combinations of catalpol with other surgical, genetic or pharmaceutical methods in the treatment of peripheral nerve injury and related diseases are also warranted to confirm.

In conclusion, catalpol not only promotes sciatic nerve axonal outgrowth and reinnervation after injury but also inhibits apoptosis in the spinal cord connected to the injured sciatic nerve. The cytoprotective and axon growth-promoting effects of catalpol following SNCI in mice are related to the activation of Akt/mTOR pathway and its modulation of BDNF and PTEN expression.

Acknowledgements

Disclosure of conflict of interest

None.

Address correspondence to: Dr. Dong Wan, Department of Emergency and Critical Care Medicine, The First Affiliated Hospital of Chongqing Medical University, Chongqing 400016, China. Tel: +86-13996012837; E-mail: wandongcqykdx@126.com

References

[1]   Panagopoulos GN, Megaloikonomos PD and Mavrogenis AF. The present and future for peripheral nerve regeneration. Orthopedics 2017; 40: e141-e156.

[2]   Navarro X. Functional evaluation of peripheral nerve regeneration and target reinnervation in animal models: a critical overview. Eur J Neurosci 2016; 43: 271-286.

[3]   Russo TL, Peviani SM, Durigan JL and Salvini TF. Electrical stimulation increases matrix metalloproteinase-2 gene expression but does not change its activity in denervated rat muscle. Muscle Nerve 2008; 37: 593-600.

[4]   Abe N, Borson SH, Gambello MJ, Wang F and Cavalli V. Mammalian target of rapamycin (mTOR) activation increases axonal growth capacity of injured peripheral nerves. J Biol Chem 2010; 285: 28034-28043.

[5]   Park KK, Liu K, Hu Y, Smith PD, Wang C, Cai B, Xu B, Connolly L, Kramvis I, Sahin M and He Z. Promoting axon regeneration in the adult CNS by modulation of the PTEN/mTOR pathway. Science 2008; 322: 963-966.

[6]   Chan KM, Gordon T, Zochodne DW and Power HA. Improving peripheral nerve regeneration: from molecular mechanisms to potential therapeutic targets. Exp Neurol 2014; 261: 826-835.

[7]   Chang IA, Lim HD, Kim KJ, Shin H and Namgung U. Enhanced axonal regeneration of the injured sciatic nerve by administration of Buyang Huanwu decoction. J Ethnopharmacol 2016; 194: 626-634.

[8]   Chiarotto GB, Drummond L, Cavarretto G, Bombeiro AL and de Oliveira AL. Neuroprotective effect of tempol (4 hydroxy-tempo) on neuronal death induced by sciatic nerve transection in neonatal rats. Brain Res Bull 2014; 106: 1-8.

[9]   Du JS, Zhao Q, Zhang YL, Wang Y and Ma M. 7,8-dihydroxycoumarin may promote sciatic nerve regeneration by suppressing NF-kappaB expression in mice. Mol Med Rep 2013; 8: 1525-1530.

[10]   Zukor K, Belin S, Wang C, Keelan N, Wang X and He Z. Short hairpin RNA against PTEN enhances regenerative growth of corticospinal tract axons after spinal cord injury. J Neurosci 2013; 33: 15350-15361.

[11]   Liu J, He QJ, Zou W, Wang HX, Bao YM, Liu YX and An LJ. Catalpol increases hippocampal neuroplasticity and up-regulates PKC and BDNF in the aged rats. Brain Res 2006; 1123: 68-79.

[12]   Dong W, Xian Y, Yuan W, Huifeng Z, Tao W, Zhiqiang L, Shan F, Ya F, Hongli W, Jinghuan W, Lei Q, Li Z and Hongyi Q. Catalpol stimulates VEGF production via the JAK2/STAT3 pathway to improve angiogenesis in rats' stroke model. J Ethnopharmacol 2016; 191: 169-179.

[13]   Liu JY, Zheng CZ, Hao XP, Zhang DJ, Mao AW and Yuan P. Catalpol ameliorates diabetic atherosclerosis in diabetic rabbits. Am J Transl Res 2016; 8: 4278-4288.

[14]   Liu YR, Lei RY, Wang CE, Zhang BA, Lu H, Zhu HC and Zhang GB. Effects of catalpol on ATPase and amino acids in gerbils with cerebral ischemia/reperfusion injury. Neurol Sci 2014; 35: 1229-1233.

[15]   Xia Z, Zhang R, Wu P, Xia Z and Hu Y. Memory defect induced by beta-amyloid plus glutamate receptor agonist is alleviated by catalpol and donepezil through different mechanisms. Brain Res 2012; 1441: 27-37.

[16]   Zhang XL, An LJ, Bao YM, Wang JY and Jiang B. d-galactose administration induces memory loss and energy metabolism disturbance in mice: protective effects of catalpol. Food Chem Toxicol 2008; 46: 2888-2894.

[17]   Zhu H, Wang Y, Liu Z, Wang J, Wan D, Feng S, Yang X and Wang T. Antidiabetic and antioxidant effects of catalpol extracted from Rehm-

annia glutinosa (Di Huang) on rat diabetes induced by streptozotocin and high-fat, high-sugar feed. Chin Med 2016; 11: 25.

[18] Cai Q, Ma T, Li C, Tian Y and Li H. Catalpol protects pre-myelinating oligodendrocytes against ischemia-induced oxidative injury through ERK1/2 signaling pathway. Int J Biol Sci 2016; 12: 1415-1426.

[19] Li DQ, Bao YM, Li Y, Wang CF, Liu Y and An LJ. Catalpol modulates the expressions of Bcl-2 and Bax and attenuates apoptosis in gerbils after ischemic injury. Brain Res 2006; 1115: 179-185.

[20] Li Y, Bao Y, Jiang B, Wang Z, Liu Y, Zhang C and An L. Catalpol protects primary cultured astrocytes from in vitro ischemia-induced damage. Int J Dev Neurosci 2008; 26: 309-317.

[21] Wang Z, Liu Q, Zhang R, Liu S, Xia Z and Hu Y. Catalpol ameliorates beta amyloid-induced degeneration of cholinergic neurons by elevating brain-derived neurotrophic factors. Neuroscience 2009; 163: 1363-1372.

[22] Yuan CX, Chu T, Liu L, Li HW, Wang YJ, Guo AC and Fan YP. Catalpol induces oligodendrocyte precursor cell-mediated remyelination in vitro. Am J Transl Res 2015; 7: 2474-2481.

[23] Zhu HF, Wan D, Luo Y, Zhou JL, Chen L and Xu XY. Catalpol increases brain angiogenesis and up-regulates VEGF and EPO in the rat after permanent middle cerebral artery occlusion. Int J Biol Sci 2010; 6: 443-453.

[24] Raducan A, Mirica S, Duicu O, Raducan S, Muntean D, Fira-Mladinescu O and Lighezan R. Morphological and functional aspects of sciatic nerve regeneration after crush injury. Rom J Morphol Embryol 2013; 54: 735-739.

[25] Chen HC, Fong TH, Hsu PW and Chiu WT. Multifaceted effects of rapamycin on functional recovery after spinal cord injury in rats through autophagy promotion, anti-inflammation, and neuroprotection. J Surg Res 2013; 179: e203-210.

[26] de Medinaceli L, Freed WJ and Wyatt RJ. An index of the functional condition of rat sciatic nerve based on measurements made from walking tracks. Exp Neurol 1982; 77: 634-643.

[27] Evans PJ, Mackinnon SE, Best TJ, Wade JA, Awerbuck DC, Makino AP, Hunter DA and Midha R. Regeneration across preserved peripheral nerve grafts. Muscle Nerve 1995; 18: 1128-1138.

[28] Kobayashi H, Miyahara K, Kusafuka J, Yamataka A, Lane GJ, Sueyoshi N, Miyano T and Puri P. A new rapid acetylcholinesterase staining kit for diagnosing Hirschsprung's disease. Pediatr Surg Int 2007; 23: 505-508.

[29] Mu L and Sanders I. Human tongue neuroanatomy: nerve supply and motor endplates. Clin Anat 2010; 23: 777-791.

[30] Witherspoon JW, Smirnova IV and McIff TE. Improved gold chloride staining method for anatomical analysis of sensory nerve endings in the shoulder capsule and labrum as examples of loose and dense fibrous tissues. Biotech Histochem 2014; 89: 355-370.

[31] Witherspoon JW, Smirnova IV and McIff TE. Neuroanatomical distribution of mechanoreceptors in the human cadaveric shoulder capsule and labrum. J Anat 2014; 225: 337-345.

[32] Schneider CA, Rasband WS and Eliceiri KW. NIH Image to ImageJ: 25 years of image analysis. Nat Methods 2012; 9: 671-675.

[33] Batt J, Bain J, Goncalves J, Michalski B, Plant P, Fahnestock M and Woodgett J. Differential gene expression profiling of short and long term denervated muscle. FASEB J 2006; 20: 115-117.

[34] Monte-Raso VV, Barbieri CH, Mazzer N, Yamasita AC and Barbieri G. Is the Sciatic Functional Index always reliable and reproducible? J Neurosci Methods 2008; 170: 255-261.

[35] Mar FM, Bonni A and Sousa MM. Cell intrinsic control of axon regeneration. EMBO Rep 2014; 15: 254-263.

[36] Grynspan D, Giassi AC, Cadonic R, Schock SC, Perozzo A, Staines WA and Bettolli M. Growth-associated protein 43 expression in ganglionic and aganglionic colon. Pediatr Dev Pathol 2012; 15: 428-429.

[37] Morita S and Miyata S. Synaptic localization of growth-associated protein 43 in cultured hippocampal neurons during synaptogenesis. Cell Biochem Funct 2013; 31: 400-411.

[38] Christie KJ and Zochodne D. Peripheral axon regrowth: new molecular approaches. Neuroscience 2013; 240: 310-324.

[39] Sun G, Li Z, Wang X, Tang W and Wei Y. Modulation of MAPK and Akt signaling pathways in proximal segment of injured sciatic nerves. Neurosci Lett 2013; 534: 205-210.

[40] Cai Q, Yao Z and Li H. Catalpol promotes oligodendrocyte survival and oligodendrocyte progenitor differentiation via the Akt signaling pathway in rats with chronic cerebral hypoperfusion. Brain Res 2014; 1560: 27-35.

[41] Hu L, Sun Y and Hu J. Catalpol inhibits apoptosis in hydrogen peroxide-induced endothelium by activating the PI3K/Akt signaling pathway and modulating expression of Bcl-2 and Bax. Eur J Pharmacol 2010; 628: 155-163.

[42] Hay N and Sonenberg N. Upstream and downstream of mTOR. Genes Dev 2004; 18: 1926-1945.

[43] Lindsay RM. Role of neurotrophins and trk receptors in the development and maintenance of sensory neurons: an overview. Philos Trans R Soc Lond B Biol Sci 1996; 351: 365-373.

[44] Singh B, Singh V, Krishnan A, Koshy K, Martinez JA, Cheng C, Almquist C and Zochodne DW. Regeneration of diabetic axons is enhanced by selective knockdown of the PTEN gene. Brain 2014; 137: 1051-1067.

[45] Christie KJ, Webber CA, Martinez JA, Singh B and Zochodne DW. PTEN inhibition to facilitate intrinsic regenerative outgrowth of adult peripheral axons. J Neurosci 2010; 30: 9306-9315.

[46] Das F, Ghosh-Choudhury N, Dey N, Mandal CC, Mahimainathan L, Kasinath BS, Abboud HE and Choudhury GG. Unrestrained mammalian target of rapamycin complexes 1 and 2 increase expression of phosphatase and tensin homolog deleted on chromosome 10 to regulate phosphorylation of Akt kinase. J Biol Chem 2012; 287: 3808-3822.

[47] Dobashi Y, Watanabe Y, Miwa C, Suzuki S and Koyama S. Mammalian target of rapamycin: a central node of complex signaling cascades. Int J Clin Exp Pathol 2011; 4: 476-495.